

# Survival Analysis on Rare Events Using Group-Regularized Multi-Response Cox Regression

Ruilin Li<sup>\*1</sup>, Yosuke Tanigawa<sup>2</sup>, Johanne M. Justesen<sup>2</sup>, Jonathan Taylor<sup>3</sup>, Trevor Hastie<sup>2,3</sup>,  
Robert Tibshirani<sup>†2,3</sup> and Manuel A. Rivas<sup>‡2</sup>

<sup>1</sup>Institute for Computational and Mathematical Engineering, Stanford University

<sup>2</sup>Department of Biomedical Data Science, Stanford University

<sup>3</sup>Department of Statistics, Stanford University

## Abstract

We propose a Sparse-Group regularized Cox regression method to improve the prediction performance of large-scale and high-dimensional survival data with few observed events. Our approach is applicable when there is one or more other survival responses that 1. has a large number of observed events; 2. share a common set of associated predictors with the rare event response. This scenario is common in the UK Biobank (Sudlow et al. 2015) dataset where records for a large number of common and rare diseases of the same set of individuals are available. By analyzing these responses together, we hope to achieve higher prediction performance than when they are analyzed individually. To make this approach practical for large-scale data, we developed an accelerated proximal gradient optimization algorithm as well as a screening procedure inspired by Qian et al. (2019). We provide a software implementation of the proposed method and demonstrate its efficacy through simulations and applications to UK Biobank data.

Cox proportional hazard model; Sparse-Group Lasso; Multi-response regression.

## 1 Introduction

### 1.1 Cox Proportional Hazard Model

Cox model (Cox 1972) provides a flexible mathematical framework that describes the relationship between the predictors and a time-to-event response. For each individual we observe a triple  $\{O, X, T\}$ , where  $X \in \mathbb{R}^d$  are the features and  $O \in \{0, 1\}$  is a status indicator. If  $O = 1$ , then  $T$  is the actual time-to-event. If  $O = 0$ , then we only know that the time-to-event is at least  $T$ . The hazard function according to the Cox model can be written as

$$h(t|X) = h_0(t) \exp(X^T \beta),$$

where  $\beta \in \mathbb{R}^d$  is the coefficients vector that measures the strength of association between  $X$  and the response. This hazard function is equivalent to the cumulative distribution function:

$$P(T \leq t|X) = 1 - \exp\left(-\int_0^t h_0(s) e^{\beta^T X} ds\right).$$

---

\*Corresponding author: [ruilinli@stanford.edu](mailto:ruilinli@stanford.edu)

†Corresponding author: [tibs@stanford.edu](mailto:tibs@stanford.edu)

‡Corresponding author: [mrivas@stanford.edu](mailto:mrivas@stanford.edu)

25 Here  $h_0 : \mathbb{R}^+ \mapsto \mathbb{R}^+$  is the baseline hazard function. In our applications we are interested in the  
 26 relationship between the features and the responses, so the baseline hazard function is a nuisance  
 27 variable. We can estimate the parameters  $\beta$  directly without knowing the baseline hazard by maxi-  
 28 mizing the log partial likelihood function (Cox 1972):

$$\begin{aligned} l(\beta|Data) &= \log \left[ \prod_{i:O_i=1} \frac{\exp(X_i^T \beta)}{\sum_{j:T_j \geq T_i} \exp(X_j^T \beta)} \right] \\ &= \sum_{i=1}^n O_i \left[ X_i^T \beta - \log \left( \sum_{j:T_j \geq T_i} \exp(X_j^T \beta) \right) \right] \end{aligned}$$

29 When the number of observed events is small relative to  $n$ , estimating  $\beta$  becomes challenging. This  
 30 could happen, for example, when the time-to-event response is the age of diagnosis of a rare disease.  
 31 In particular, if  $O_i$  are i.i.d Bernoulli random variables with probability  $p$ , then the information  
 32 matrix is proportional to  $p$  and thus the asymptotic variance of the maximum partial likelihood  
 33 estimate is inversely proportional to  $p$ .

34 We evaluate a fitted survival model using the concordance index, or the C-index. For a param-  
 35 eter estimate  $\hat{\beta}$ , the C-index is defined as

$$C(\hat{\beta}) = \frac{\sum_{i=1}^n O_i (|\{j : \hat{\beta}^T X_i > \hat{\beta}^T X_j\}| + |\{j : \hat{\beta}^T X_i = \hat{\beta}^T X_j\}|/2)}{\sum_{i=1}^n O_i |\{j : T_j > T_i\}|}. \quad (1)$$

37 For more details on C-index, see Harrell et al. (1982), Li et al. (2020).

## 38 1.2 Sparse-Group Lasso

39 The Lasso method (Tibshirani 1996) makes the assumption that only a small subset of predictors are  
 40 associated with the response. In other words, it assumes that  $\beta$  has only a small number of non-zero  
 41 entries. A sparse solution can be obtained by optimizing an  $L_1$ -regularized objective function.

42 Sparse-Group Lasso (Simon et al. 2013) assumes not only that many individual elements of  $\beta$  are  
 43 0, but also that many groups of variables have coefficients 0 simultaneously. For example, in a  
 44 single-response Cox model with  $d$ -dimensional features, if groups of variables  $\mathcal{G} = \{g : g \subseteq [d]\}$   
 45 are believed to have sparse-group structure, then the sparse-group Lasso minimizes the following  
 46 objective function:  
 47

$$-\sum_{i=1}^n O_i \left[ X_i^T \beta - \log \left( \sum_{j:T_j \geq T_i} \exp(X_j^T \beta) \right) \right] + \lambda \|\beta\|_1 + \sum_{g \in \mathcal{G}} \lambda_g \|\beta_g\|_2. \quad (2)$$

## 48 2 Methods

### 49 2.1 Preliminaries

50 In this section we define the notations and the key model assumptions that we will use in the  
 51 subsequent sections. For an integer  $n$ , define  $[n] = \{1, 2, \dots, n\}$  and define  $x_+ = \max\{x, 0\}$  for all  
 52  $x \in \mathbb{R}$ .

We analyze  $K \geq 1$  time-to-event responses on  $n$  individuals. For example, the responses could  
 be time from birth to  $K$  different diseases. The data we observed are in the format:

$$\mathcal{D} = \{X_i, T_i^1, \dots, T_i^K, O_i^1, \dots, O_i^K\}_{i=1}^n.$$

53 Here  $X_i \in \mathbb{R}^d$  are  $i$ th individual's features. Denote the full features matrix  $\mathbf{X} = [X_1, X_2, \dots, X_n]^T \in$   
 54  $\mathbb{R}^{n \times d}$ . For  $k = 1, \dots, K$ ,  $O_i^k = 1$  implies that  $T_i^k$  is the true time until the event  $k$  and for the  $i$ th  
 55 individual, and  $O_i^k = 0$  implies that the true time until the event  $k$  is right-censored at  $T_i^k$ . We  
 56 assume each response follows a Cox proportional hazard model:

$$h_k(t|X) = h_{0,k}(t) \exp(X^T \beta_k). \quad (3)$$

where  $h_{0,k} : \mathbb{R}^+ \mapsto \mathbb{R}^+$  is the baseline hazard function of the  $k$ th response. Let

$$n_k = \sum_{i=1}^n O_i^k$$

57 be the number of observed event  $k$ .

58 We make the assumption that not only  $\beta_k$  is sparse for all  $k \in [K]$ , but they also have a small  
 59 common support. That is  $\{j \in [d] : \beta_k^j \neq 0, k \in [K]\}$  is a small set relative to  $d$ . In human  
 60 genetics applications, the first assumption means that each response is associated with a small set  
 61 of genetic variants, and the second assumption implies that there are significant overlap among the  
 62 genetic variants that are associated with each response. This belief is the main driver for prediction  
 63 performance improvements on rare diseases, and it translates to the following regularized partial  
 64 likelihood objective function:

$$\min_{\beta_1, \dots, \beta_K} \sum_{k=1}^K \frac{1}{n_k} \left[ \sum_{i: O_i^k=1} -\beta_k^T X_i + \log \left( \sum_{j: T_j^k \geq T_i^k} \exp(\beta_k^T X_j) \right) \right] + \lambda \left( \sum_{j=1}^d \|\beta^j\|_1 + \alpha \|\beta^j\|_2 \right). \quad (4)$$

Here the first term is the sum of the  $K$  negative log-partial-likelihood, normalized by the number  
 of observed events. The second term is the regularization.  $\|\beta^j\|_1$ ,  $\|\beta^j\|_2$  are the 1-norm and 2-  
 norm of the coefficients for the  $j$ th variable. That is, if we put all the parameters into a matrix  
 $B = [\beta_1, \beta_2, \dots, \beta_K] \in \mathbb{R}^{d \times K}$ , then  $\beta^j$  is the  $j$ th row of  $B$  and  $\beta_k$  is the  $k$ th column. Note that  
 when  $\alpha = 0$ , the objective function decouples for each  $\beta_k$  and they can be optimized separately. In  
 our implementation we solve a slightly more general problem:

$$\min_{\beta_1, \dots, \beta_K} \left\{ \sum_{k=1}^K \frac{1}{n_k} \left[ \sum_{i: O_i^k=1} -\beta_k^T X_i + \log \left( \sum_{j: T_j^k \geq T_i^k} \exp(\beta_k^T X_j) \right) \right] + \lambda \left[ \sum_{j=1}^d w_j (\|\beta^j\|_1 + \alpha \|\beta^j\|_2) \right] \right\},$$

65 where  $\{w_j\}_{j=1}^d$  are user provided penalty factor for each variables, which may be useful in the set-  
 66 ting where protein-truncating or protein-altering variants should be prioritized (Rivas et al. 2015,  
 67 DeBoever et al. 2018). Just like in Yuan & Lin (2006), our implementation by default fixes  $\alpha$  at  
 68  $\sqrt{K}$ . The solution is computed on a pre-defined sequence of  $\lambda$ s:  $\lambda_1 > \lambda_2 > \dots > \lambda_L$ , where  $\lambda_1$  is  
 69 chosen so that the solution just become non-zero.

70

71 To simplify the notation, for  $j \in [d]$  denote

$$g_j = g_j(\beta_1, \dots, \beta_K) := \frac{\partial}{\partial \beta^j} \sum_{k=1}^K \frac{1}{n_k} \left[ \sum_{i: O_i^k=1} -\beta_k^T X_i + \log \left( \sum_{j: T_j^k \geq T_i^k} \exp(\beta_k^T X_j) \right) \right]. \quad (5)$$

Here  $g_j \in \mathbb{R}^K$  is the partial derivative of the smooth part of (4) with respect to the coefficients of  
 the variable  $j$ . Finally, let  $S_1(\cdot; \lambda) : \mathbb{R}^K \mapsto \mathbb{R}^K$  be the element-wise soft-thresholding function:

$$S_1(v; \lambda)_k = \text{sign}(v_k)(|v_k| - \lambda)_+ \text{ for all } k \in [K].$$

## 72 2.2 Optimization Method

73 We use a Nesterov-accelerated (Nesterov 1983) proximal gradient method (Daubechies et al. 2004,  
74 Beck & Teboulle 2009) to optimize the objective function (4). Proximal gradient algorithm is  
75 particularly suitable when the objective function is the sum of a smooth function and a simple  
76 function. In our case the smooth function is the sum of the negative log-partial-likelihood functions,  
77 and the simple function is the regularization term. The algorithm alternates between two steps until  
78 convergence criteria is met:

1. A gradient step that decreases the smooth part of the objective:

$$\beta^j \leftarrow \beta^j - tg_j,$$

79 where  $t$  is the step size that we determine using backtracking line search.

2. A proximal step that keeps the regularization term small:

$$\beta^j \leftarrow \text{prox}_t(\beta^j).$$

Here the proximal operator  $\text{prox}_t : \mathbb{R}^K \mapsto \mathbb{R}^K$  is defined as

$$\text{prox}_t(x) := \arg \min_z \frac{1}{2t} \|z - x\|_2^2 + \lambda \|z\|_1 + \lambda \alpha \|z\|_2.$$

To simplify the notation we omit the dependency of  $\text{prox}_t(x)$  on  $\lambda, \alpha$ . Simple calculation shows that

$$\text{prox}_t(x) = S_2(S_1(x; t\lambda); t\alpha\lambda).$$

where  $S_2(\cdot; t\alpha\lambda) : \mathbb{R}^K \mapsto \mathbb{R}^K$  is a group soft-thresholding operator:

$$S_2(v; t\alpha\lambda) = \begin{cases} 0 & \text{if } \|v\|_2 \leq t\alpha\lambda \\ \frac{v}{\|v\|_2} (\|v\|_2 - t\alpha\lambda) & \text{otherwise} \end{cases}.$$

80 We describe the optimization algorithm in pseudocode, including details about Nesterov acceleration  
81 and backtracking line search in algorithm 1.

## 82 2.3 Variable Screening for Lasso Path

83 In many of our applications the data is large-scale and high-dimensional. For example, the UK  
84 Biobank dataset (Sudlow et al. 2015) contains millions of genetic variants and over 500,000 partici-  
85 pants. Reading the feature matrix of the UK Biobank dataset into R requires more than 4 terabytes  
86 of memory, which is much larger than the RAM size of most computers. While memory mapping  
87 (Kane et al. 2013) allows users to access out-of-memory data with ease, it requires lots of disk In-  
88 put/Output operations, which is much slower than in-memory operation. This becomes even more  
89 problematic for iterative optimization algorithms that use the entire feature matrix every iteration.

90  
91 To reduce the frequency of reading the full data matrix, here we derive a version of variable screening  
92 method following similar ideas of the strong rule (Tibshirani et al. 2012) and the Batch Screening  
93 Iterative Lasso (Qian et al. 2019).

94  
95 For each  $\alpha > 0, v \in \mathbb{R}^K$ , define the  $\alpha^*$  norm of  $v$  to be

$$\|v\|_{\alpha^*} := \sup\{u^T v : u \in \mathbb{R}^K, \|u\|_1 + \alpha \|u\|_2 \leq 1\}. \quad (6)$$

96 We use the following results to get an optimality condition for the solutions  $\beta_1, \dots, \beta_K$ . The proofs  
97 are given in section 6.

---

**Algorithm 1:** Proximal Gradient Method for (4)

---

Set line search parameter  $\eta > 1$ ;

Denote the parameter matrix  $B \in \mathbb{R}^{d \times K}$ . Initialize  $B^{(0)}$ ;

Write the smooth part of the objective as:

$$f(B) = \sum_{k=1}^K \frac{1}{n_k} \left[ \sum_{i:O_i^k=1} -\beta_k^T X_i + \log \left( \sum_{j:T_j^k \geq T_i^k} \exp(\beta_k^T X_j) \right) \right].$$

Set iteration count  $i = 0$ ; Set initial step-size  $t = 1$ ; Set Nesterov weights  $w_0, w_1 = 1$ ;

**while**  $B$  has not converged **do**

Nesterov acceleration:  $w_1 \leftarrow (1 + \sqrt{1 + 4w_0^2})/2$ ;

$B^{(i+0.5)} \leftarrow B^{(i)} + (w_0 - 1)(B^{(i)} - B^{(i-1)})/w_1$ ;  $w_0 \leftarrow w_1$ ;

Compute the gradient  $g_j = \frac{\partial}{\partial \beta^j} f(B^{(i+0.5)})$  for  $j \in [d]$ ;

Start backtracking line search:

**repeat**

$B \leftarrow B^{(i+0.5)} - t \nabla f(B^{(i+0.5)})$ ;

Denote  $\beta^j$  the  $j$ th row of  $B$  for  $j \in [d]$ ;

Apply proximal step:  $\beta^j \leftarrow \text{prox}_t(\beta^j)$  for  $j \in [d]$ ;

**if**  $f(B) \leq f(B^{(i+0.5)}) + \langle B - B^{(i+0.5)}, \nabla f(B^{(i+0.5)}) \rangle + \|B - B^{(i+0.5)}\|_2^2/(2t)$  **then**

| **break**;

**end**

$t \leftarrow t/\eta$ ;

**until** the break condition above is satisfied;

$B^{(i+1)} \leftarrow B$ ;  $i \leftarrow i + 1$ ;

Check convergence based on objective value change or parameter change.

**end**

**return**  $B^{(i)}$

---

98 **Proposition 1.** For any  $\lambda > 0$ , the gradients defined at (5) at the optimal solution to (4) satisfies:

$$\|g_j\|_{\alpha^*} \begin{cases} \leq \lambda & \text{if the optimal } \beta^j = 0 \\ = \lambda & \text{if the optimal } \beta^j \neq 0 \end{cases} \text{ for all } j \in [d]. \quad (7)$$

99

100 This result motivates us to first fit a model (solving (4)) using a small number of variables whose  
101 gradient has the largest  $\alpha^*$  norm, assuming the coefficients for the rest of the variables are all zero.  
102 Then to verify the validity of the assumption we check that  $\|g_j\|_{\alpha^*} \leq \lambda$  for variables assumed to  
103 have zero coefficients. We refer to this step as KKT checking. Note that based on its definition (6),  
104 it's not clear how we can compute  $\|v\|_{\alpha^*}$ . Here we give a more explicit characterization.

105 **Proposition 2.**  $\|v\|_{\alpha^*} \leq \lambda$  if and only if  $\|S_1(v; \lambda)\|_2 \leq \alpha\lambda$ .

106 Using the above we can check if  $\|v\|_{\alpha^*} \leq \lambda$  quite easily and compute  $\|v\|_{\alpha^*}$  using binary search  
107 in  $\mathcal{O}(K \log \|v\|_{\infty})$  to any fixed precision (since  $\|v\|_{\alpha^*} \leq \|v\|_{\infty}$ ).

108

109 Now we are ready to state the overall structure of our algorithm with variable screening. Sup-  
110 pose valid solutions for  $\lambda_1, \dots, \lambda_l$  have been obtained. Next we follow these steps:

111 1. (**Screening**) In the last iteration, we cache the full gradient  $\{g^j\}_{j=1}^d$  evaluated at the solution  
112 at  $\lambda_l$ . In the fitting step we include two types of variables:

- 113 • We include the ever-active variables  $\mathcal{A} := \{j \in [d] : \hat{\beta}^j \neq 0 \text{ for any previously obtained } \hat{\beta}\}$ .
- 114 • Top  $M$  variables with the largest  $\|g_j\|_{\alpha^*}$  that are also not ever-active.

115 We denote the set of variables used to fit (4) as the strong set  $\mathcal{S} \subseteq [d]$ .

116 2. (**Fitting**) In this step, we solve the problem (4) for the next few  $\lambda$ s using only variables in  $\mathcal{S}$ ,  
117 assuming  $\beta^j = 0$  for all  $j \notin \mathcal{S}$ . This is done using proximal gradient descent (algorithm 1).  
118 To speed-up the computation we initialize the variables at the previous valid solution (warm  
119 start).

120 3. (**KKT Checking**) After obtaining the solution from the fitting step. We compute the full  
121 gradient. This is the only step we will need the full data matrix  $\mathbf{X}$ . We check if the KKT  
122 conditions (7) are satisfied for all variables then go back to the screening step at the first  $\lambda$   
123 value where the KKT condition fails. We also cache the full gradient at the last valid solutions  
124 for the screening step.

125 4. (**Early Stopping**) We keep a separate validation set to evaluate the current estimated pa-  
126 rameters. We choose the optimal  $\lambda$  as the one that gives the highest validation C-index. The  
127 optimal  $\lambda$  might be different for different responses. In this paper we focus only on the predic-  
128 tion accuracy of one rare event, so it is reasonable to stop when the validation C-index of this  
129 response starts to decrease, regardless if the optimal  $\lambda$  for other responses has been reached.

130 These steps are described in algorithm 2.

## 131 2.4 Software

132 We implemented the proximal gradient method in section 2.1 as an R package, available at <https://github.com/rivas-lab/multispnet-Cox>. In this package we also implement the screening pro-  
133 cedure described in this section for genetics data in Plink2 format (Chang et al. 2014).  
134

135

---

**Algorithm 2:** Iterative Screening for Lasso Path

---

Initialize ever active set  $\mathcal{A}^{(0)} = \emptyset$  and construct the regularization parameters  $\lambda_1, \dots, \lambda_L$ ;

Initialize a short list of initial regularization parameters  $\Lambda^{(0)} = \{\lambda_1, \dots, \lambda_{L^{(0)}}\}$ ;

Initialize the parameters  $\hat{\beta}_1^{(0)}, \dots, \hat{\beta}_K^{(0)} = 0$ ; Set the iteration counter  $i = 0$ ;

**while**  $\hat{\beta}(\lambda_L)$  not computed **do**

    Set  $v$  to be the largest number such that the solutions for  $\lambda_1, \dots, \lambda_v$  are obtained;

**Screening:**

    Compute (or use the cached) full gradient (5)  $g_1, \dots, g_d$  at the last solutions.

    Set  $\mathcal{E}_M^{(i)}$  to be the  $M$  variables in  $[d] \setminus \mathcal{A}^{(i)}$  with the largest  $\|g_j\|_{\alpha^*}$ ;

    Set  $\mathcal{S}^{(i)} = \mathcal{A}^{(i)} \cup \mathcal{E}_M^{(i)}$ . This will be the variables used in the fitting step;

**Fitting:**

**for**  $\lambda \in \Lambda^{(i)}$  **do**

        Obtain parameter estimates by solving (4) using only variables in  $\mathcal{S}^{(i)}$ ;

        The optimization algorithm is described in algorithm 2;

        Coefficients for variables not in  $\mathcal{S}^{(i)}$  are set to be zero.;

**end**

**Checking:**

    Compute the full gradients  $g_1(\lambda), \dots, g_d(\lambda)$  at solutions obtained with regularization parameters  $\lambda \in \Lambda^{(i)}$ ;

    Find the smallest  $\lambda \in \Lambda^{(i)}$  such that the KKT condition (7) is satisfied:

$$\bar{\lambda}^{(i)} = \min \left\{ \lambda \in \Lambda^{(i)} : \max_{j \in [d] \setminus \mathcal{S}^{(i)}} \|g_j(\lambda)\|_{\alpha^*} < \lambda \right\}$$

    Update ever active set  $\mathcal{A}^{(i+1)} = \mathcal{A}^{(i)} \cup \{j : \hat{\beta}^j(\bar{\lambda}^{(i)}) \neq 0\}$ ;

    Update  $\Lambda^{(i+1)} = \{\lambda \in \Lambda^{(i)} : \lambda < \bar{\lambda}^{(i)}\}$ . Extend  $\Lambda^{(i+1)}$  if it is too short.;

    For  $\lambda \in \{\lambda \in \Lambda^{(i)} : \lambda \geq \bar{\lambda}^{(i)}\}$ , we obtain valid solutions; Set  $i = i + 1$ ;

**end**

**return**  $\hat{\beta}(\lambda_1), \dots, \hat{\beta}(\lambda_L)$

---

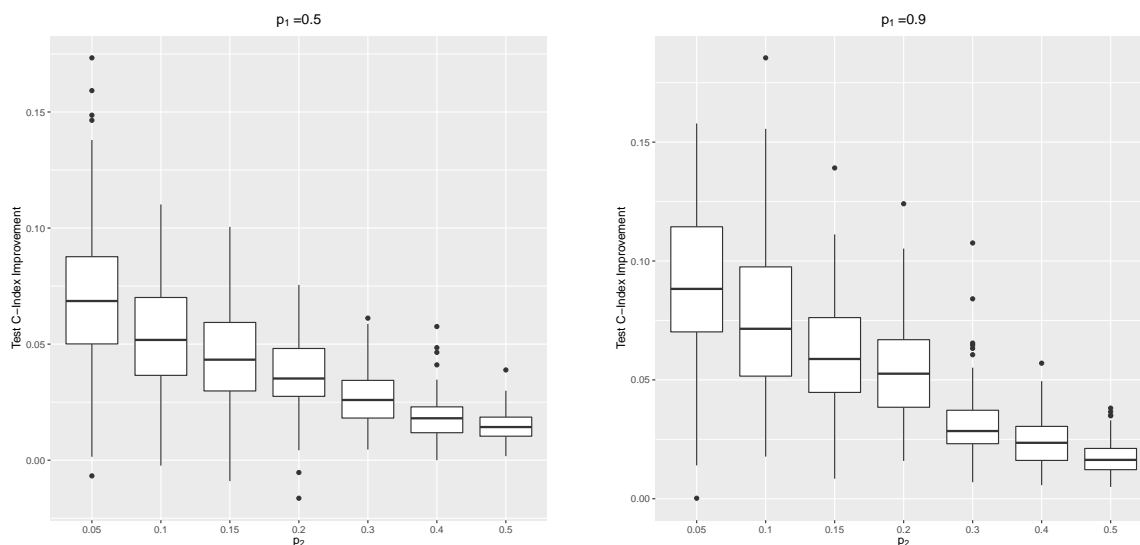


Figure 1: Absolute improvements in test C-index of the rare event response when two responses are trained together.  $p_1$  is the proportion of uncensored events of the first response.  $p_2$  (rare) is the proportion of uncensored events of the second response. The true coefficients have exactly the same support.

136 The major computational bottleneck in the proximal gradient method are matrix-matrix multiplica-  
 137 tions. These operations have high arithmetic intensity and are particularly suitable for GPU accel-  
 138 eration. Therefore we also provide a GPU implementation of algorithm 1 on CUDA-enabled device,  
 139 available at [https://github.com/rivas-lab/multispnet-Cox\\_gpu](https://github.com/rivas-lab/multispnet-Cox_gpu). With  $n = d = 10000$ ,  $K =$   
 140  $20$ , the GPU implementation achieves almost  $10\times$  speedup in solving a path of  $50$   $\lambda$ s (9.7 seconds vs  
 141 92 seconds) on a Tesla V100 GPU than the CPU implementation on an Intel Xeon 6528R processor  
 142 with 28 threads, accelerated using Intel’s Math Kernel Library.

### 143 3 Simulations

144 In this section we compare the performance of the proposed approach against a simple Lasso,  
 145 where multiple responses are fitted independently. Here we simulate two responses ( $K = 2$ ),  
 146  $n = 400$ ,  $d = 5000$ , the entries of the predictor matrix are i.i.d random signs  $\{-1, 1\}$  with prob-  
 147 ability 0.5 each, and the time-to-event responses are exponential distributed with rate  $\exp(X_i^T \beta)$ ,  
 148 which satisfies proportional hazard. The parameters  $\beta_1, \beta_2$  have a common support of size 35. We  
 149 use a large (5000 samples) and uncensored validation set to select the optimal  $\lambda$ .  $\alpha$  is fixed at  $\sqrt{2}$ .  
 150 The parameter estimate corresponding to the best  $\lambda$  is then evaluated at a large, uncensored test  
 151 set. We use the C-index as both the validation and test metric. The censoring for both responses  
 152 are randomly chosen and independent from everything else. The simulations are done for multiple  
 153 combinations of censoring proportions, each repeated 100 times. Here we report the improvement  
 154 in C-index of the response with rare events. See Figure 1.

155  
 156 The assumption that the coefficients for different responses have the same support can come from  
 157 domain knowledge (such as biology). In practice this is usually not exactly satisfied. Here we use  
 158 simulation to examine the robustness of our approach. The setup is the same as the previous sim-  
 159 ulations, except now the overlap of the support might be smaller than 35 (the number of non-zero  
 160 entries of  $\beta_1, \beta_2$ ). See the left panel of Figure 2.



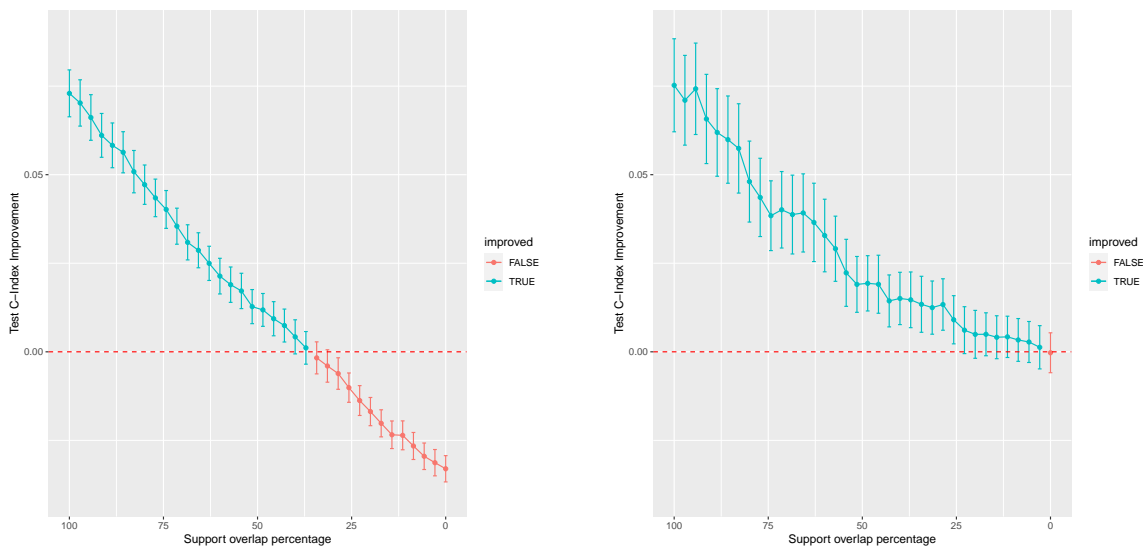


Figure 2: Absolute improvements in Test C-index of the rare event response when two responses are trained together. 60% of the events for the first response are uncensored, and 5% of the events for the second are uncensored. The horizontal axis is the overlap proportion of the support of  $\beta_1$  and  $\beta_2$ , in other words  $|\{i \in [p] : \beta_1^i \neq 0, \beta_2^i \neq 0\}| \cdot 100/35$ . The left panel shows the result when  $\alpha$  is fixed at  $\sqrt{2}$ , and  $\lambda$  is selected from a large uncensored validation set. The right panel shows the result when  $\alpha$  is selected between  $\{0, \sqrt{2}\}$  using a small validation set of size 200 with 5% uncensored second event. The whiskers indicates 95% confidence intervals.

161

162 We can see that, when the support overlap percentage is less than around 40% the prediction  
 163 performance actually becomes worse when the two responses are trained together. One solution to  
 164 this problem is to also treat  $\alpha$  as a hyperparameter and use the validation set to determine it. For  
 165 large data set having a two-dimensional hyperparameter could be quite cumbersome. In our simu-  
 166 lation and real data application, we only choose  $\alpha$  from two values  $\{0, \sqrt{K}\}$ , although in principle  
 167 one can use a large set of  $\alpha$  candidates at a higher computational cost. The right panel of Figure 2  
 168 shows the C-index improvements when we use a small validation set to determine whether  $\alpha$  should  
 169 be 0 or  $\sqrt{K}$ . All other settings are the same as above.

170

## 171 4 Application to UK Biobank Data

172 In this section we apply the proposed method to UK Biobank data. We focus on thyroiditis, which  
 173 has 808 observed events in the study population (337, 129 white British participants). We randomly  
 174 assign 70% of the samples to the training set, 10% to the validation set, and 20% to the test set. The  
 175 predictors here are  $\sim 1$  million genetic variants, as well as 11 covariates (sex, and 10 principal com-  
 176 ponents of the genetic variants). We first fit a baseline model using only the 11 covariates, without  
 177 using any genetic variants. This gives a baseline test C-index at 0.649. We then fit a single-response  
 178 Lasso Cox regression, where  $\lambda$  is selected using based on the validation C-index. At the best  $\lambda$  value,  
 179 the test C-index is 0.679. To apply our approach, we pair thyroiditis with 6 other more common  
 180 endocrine diseases that we believe share common genetic factors with thyroiditis. These diseases  
 181 are listed in the table below. Here we report the test C-indices when thyroiditis is paired with  
 182 one other disease and when all 7 responses are trained together. We also report the test C-indices

183 when we use the validation set to determine both the optimal  $\lambda$  and whether to set  $\alpha = 0$  or  $\alpha = \sqrt{K}$ .

184

185 Table 1 shows clear increase in prediction performance on thyroiditis when all 7 responses are  
186 trained together, and when thyroiditis is paired with thyrotoxicosis only. On the other hand, all  
187 multi-response solutions have test C-index comparable with the single response solution.

Paired response(s)	Test C-index	Test C-index (validate $\alpha$ )
thyroiditis (single response)	0.679	-
other hypothyroidism	<b>0.682</b>	<b>0.682</b>
other non-toxic goitre	<b>0.681</b>	0.679
thyrotoxicosis (hyperthyroidism)	<b>0.686</b>	<b>0.686</b>
other disorders of thyroid	0.679	0.679
insulin-dependent diabetes mellitus	<b>0.683</b>	<b>0.683</b>
non-insulin-dependent diabetes mellitus	0.679	0.679
all 7 responses trained together	<b>0.688</b>	<b>0.688</b>

Table 1: Test C-index of thyroiditis when this response is paired with other ones. The second column is obtained when  $\alpha$  is fixed at  $\sqrt{K}$  (which is 1 in the first row,  $\sqrt{7}$  in the last row, and  $\sqrt{2}$  in the rest). The third column is obtained when we use the validation set to choose  $\alpha$  between 0 (single-response) and  $\sqrt{K}$ . Improved C-indices are given in boldface. Baseline test C-index of thyroiditis, when only the 11 covariates are used for fitting, is 0.649.

## 188 5 Conclusion and Discussion

189 We developed a regularized regression method for multiple survival responses. This method is par-  
190 ticularly suitable when we can pair a response with few observed events with others having a larger  
191 number of events, such that these responses have a same set of useful predictors. We demonstrate  
192 the improvements in the prediction accuracy for the rare events responses through simulation and  
193 real data applications. We also provide efficient implementation for the proposed method.

194

195 Here are two directions for future studies. When there are more than two responses, the relationship  
196 between the prediction performance and the degree of overlapping in the coefficients support is yet  
197 to be understood. On the practical side, it is reasonable to have different types of models (not  
198 just Cox model), or even different response types (such as binary or count) to boost the accuracy  
199 of survival analysis on rare events. In principle the same type of regularization could still be applied.

200

201 For the GPU implementation, one challenge is the limited amount of memory available on GPUs.  
202 In modern computer clusters it is common to have machines with hundreds of Gigabytes of system  
203 memory, but most GPUs have less than 32GB of memory. In our implementation we use single pre-  
204 cision floating point numbers to store the data matrix, which alleviates memory burden by a factor  
205 of two. However, for UK Biobank scale data this is still sometimes insufficient. For example, when  
206 the number of participants in the training data is 250,000, we are only able to fit a model with up  
207 to 32,000 variables on a Tesla V100. One possible solution is to use multiple GPUs, but inter-GPU  
208 communication might become the bottleneck. For genetics data, another solution is to utilize their  
209 2-bit representation, which can significantly reduce memory requirement (2 bits per entry vs 32).

210 We leave these ideas for future studies.

## 211 6 Proof of Propositions

### 212 6.1 Proof of Proposition 1

213 We show a slightly more general result from convex analysis. Let  $f : \mathbb{R}^K \mapsto \mathbb{R}$  be continuously  
 214 differentiable, convex, and bounded from below. Let  $\|\cdot\|$  be a norm on  $\mathbb{R}^K$ , and  $\|\cdot\|_*$  be its  
 215 corresponding dual norm. Let  $\lambda > 0$ , and set

$$x^* := \arg \min_x f(x) + \lambda \|x\| \quad (8)$$

216 We will show that

$$\|\nabla f(x^*)\|_* \begin{cases} \leq \lambda & \text{if } x^* = 0 \\ = \lambda & \text{if } x^* \neq 0 \end{cases} \quad (9)$$

217 It is clear that (8) is equivalent to the constrained optimization problem

$$\min_{x,y} f(x) + \lambda \|y\| \text{ such that } x = y. \quad (10)$$

218 The Lagrangian is

$$\mathcal{L}(x, y, z) = f(x) + \lambda \|y\| + z^T(y - x). \quad (11)$$

219 The Lagrangian dual is

$$g(z) := \inf_{x,y} \mathcal{L}(x, y, z) = \inf_y \lambda \|y\| + z^T y + \inf_x f(x) - z^T x. \quad (12)$$

220 Using the definition of dual norm, when  $\|z\|_* > \lambda$ , the infimum of the first term above is  $-\infty$ , and  
 221 when  $\|z\|_* \leq \lambda$ , the infimum is 0. Therefore

$$g(z) = \begin{cases} -\infty & \text{if } \|z\|_* > \lambda \\ \inf_x f(x) - z^T x & \text{if } \|z\|_* \leq \lambda \end{cases} \quad (13)$$

222 Therefore the dual solution  $z^* := \arg \max_z g(z)$  must satisfy  $\|z\|_* \leq \lambda$ . Now we go back to the  
 223 Lagrangian. Since the primal objective is convex and Slaters condition holds, the solution to the  
 224 primal problem can be obtained through minimizing

$$\mathcal{L}(x, y, z^*) = f(x) + \lambda \|y\| + z^{*T}(y - x). \quad (14)$$

225 which implies that, at the optimal  $x^*$  we must have  $\nabla f(x^*) = z^*$ , so

$$\|\nabla f(x^*)\|_* = \|z^*\|_* \leq \lambda, \text{ and } \lambda \|x^*\| + \nabla f(x^*)^T x^* = 0 \quad (15)$$

226 If  $x^* = 0$ , then the second equality is already satisfied, so we only need  $\|\nabla f(x^*)\|_* \leq \lambda$ . If  $x^* \neq 0$ ,  
 227 then by Holder's inequality

$$\lambda \|x^*\| = |\nabla f(x^*)^T x^*| \leq \|\nabla f(x^*)\|_* \|x^*\| \leq \lambda \|x^*\|, \quad (16)$$

228 so we must have  $\|\nabla f(x^*)\|_* = \lambda$ . Proposition 1 is a direct consequence of this result.

### 229 6.2 Proof of Proposition 2

230 We prove the claim for  $\lambda = 1$ . The regularization term can be written as

$$\|u\|_1 + \alpha \|u\|_2 = \sup_{\|v_1\|_\infty \leq 1} v_1^T u + \sup_{\|v_2\|_2 \leq \alpha} v_2^T u = \sup_{v \in \mathcal{B}_\alpha^*} v^T u \quad (17)$$

231 where  $\mathcal{B}_\alpha^*$  is the unit dual ball

$$\mathcal{B}_\alpha^* := \{v_1 \in \mathbb{R}^K : \|v_1\|_\infty \leq 1\} \oplus \{v_2 \in \mathbb{R}^K : \|v_2\|_2 \leq \alpha\}. \quad (18)$$

232 That is  $\|v\|_{\alpha^*} \leq 1$  if and only if  $v \in \mathcal{B}_\alpha^*$ , which by definition means that  $v = v_1 + v_2$  for some  
233  $\|v_1\|_\infty \leq 1, \|v_2\|_2 \leq \alpha$ . We must have (and it is sufficient to have)

$$\inf_{\|v_1\|_\infty < 1} \|v - v_1\|_2 \leq \alpha. \quad (19)$$

234 The infimum on the left-hand side is achieved when  $v_1 = v - S_1(v, 1)$ , which proves the claim.

## 235 Acknowledgments

236 Y.T. is supported by Funai Overseas Scholarship from Funai Foundation for Information Technology  
237 and the Stanford University School of Medicine.

238 M.A.R. is supported by Stanford University and a National Institute of Health center for Multi  
239 and Trans-ethnic Mapping of Mendelian and Complex Diseases grant (5U01 HG009080). This work  
240 was supported by National Human Genome Research Institute (NHGRI) of the National Institutes  
241 of Health (NIH) under awards R01HG010140. The content is solely the responsibility of the authors  
242 and does not necessarily represent the official views of the National Institutes of Health.

243 R.T was partially supported by NIH grant 5R01 EB001988-16 and NSF grant 19 DMS1208164.

244 T.H. was partially supported by grant DMS-1407548 from the National Science Foundation, and  
245 grant 5R01 EB 001988-21 from the National Institutes of Health.

246 This research has been conducted using the UK Biobank Resource under application number  
247 24983. We thank all the participants in the study. The primary and processed data used to generate  
248 the analyses presented here are available in the UK Biobank access management system (<https://amsportal.ukbiobank.ac.uk/>) for application 24983, "Generating effective therapeutic hypotheses from genomic and hospital linkage data" (<http://www.ukbiobank.ac.uk/wp-content/uploads/2017/06/24983-Dr-Manuel-Rivas.pdf>), and the results are displayed in the Global Biobank Engine (<https://biobankengine.stanford.edu>).

253 Some of the computing for this project was performed on the Sherlock cluster. We would like to  
254 thank Stanford University and the Stanford Research Computing Center for providing computational  
255 resources and support that contributed to these research results.

256 *Conflict of Interest:* None declared.

## References

- 257
- 258 Beck, A. & Teboulle, M. (2009), ‘A fast iterative shrinkage-thresholding algorithm for linear inverse  
259 problems’, *SIAM J. Img. Sci.* **2**(1), 183–202.  
260 **URL:** <https://doi.org/10.1137/080716542>
- 261 Chang, C., Chow, C., Tellier, L., Vattikuti, S., Purcell, S. & Lee, J. (2014), ‘Second-generation plink:  
262 Rising to the challenge of larger and richer datasets’, *GigaScience* **4**.
- 263 Cox, D. R. (1972), ‘Regression models and life-tables’, *Journal of the Royal Statistical Society. Series*  
264 *B (Methodological)* **34**(2), 187–220.  
265 **URL:** <http://www.jstor.org/stable/2985181>
- 266 Daubechies, I., Defrise, M. & De Mol, C. (2004), ‘An iterative thresholding algorithm for linear  
267 inverse problems with a sparsity constraint’, *Communications on Pure and Applied Mathematics*  
268 **57**(11), 1413–1457.  
269 **URL:** <https://onlinelibrary.wiley.com/doi/abs/10.1002/cpa.20042>
- 270 DeBoever, C., Tanigawa, Y., Lindholm, M. E., McInnes, G., Lavertu, A., Ingelsson, E., Chang,  
271 C., Ashley, E. A., Bustamante, C. D., Daly, M. J. et al. (2018), ‘Medical relevance of protein-  
272 truncating variants across 337,205 individuals in the uk biobank study’, *Nature communications*  
273 **9**(1), 1–10.
- 274 Harrell, F. E., Califf, R. M., Pryor, D. B., Lee, K. L. & Rosati, R. A. (1982), ‘Evaluating the yield  
275 of medical tests’, *Jama* **247**(18), 2543–2546.
- 276 Kane, M., Emerson, J. & Weston, S. (2013), ‘Scalable strategies for computing with massive data’,  
277 *Journal of Statistical Software, Articles* **55**(14), 1–19.  
278 **URL:** <https://www.jstatsoft.org/v055/i14>
- 279 Li, R., Chang, C., Justesen, J. M., Tanigawa, Y., Qian, J., Hastie, T., Rivas, M. A. & Tibshirani, R.  
280 (2020), ‘Fast Lasso method for large-scale and ultrahigh-dimensional Cox model with applications  
281 to UK Biobank’, *Biostatistics* . kxaa038.  
282 **URL:** <https://doi.org/10.1093/biostatistics/kxaa038>
- 283 Nesterov, Y. (1983), A method for solving the convex programming problem with convergence rate  
284  $O(1/k^2)$ .
- 285 Qian, J., Du, W., Tanigawa, Y., Aguirre, M., Tibshirani, R., Rivas, M. A. & Hastie, T. (2019), ‘A  
286 fast and flexible algorithm for solving the lasso in large-scale and ultrahigh-dimensional problems’,  
287 *bioRxiv* .  
288 **URL:** <https://www.biorxiv.org/content/early/2019/05/07/630079>
- 289 Rivas, M. A., Pirinen, M., Conrad, D. F., Lek, M., Tsang, E. K., Karczewski, K. J., Maller, J. B.,  
290 Kukurba, K. R., DeLuca, D. S., Fromer, M. et al. (2015), ‘Effect of predicted protein-truncating  
291 genetic variants on the human transcriptome’, *Science* **348**(6235), 666–669.
- 292 Simon, N., Friedman, J., Hastie, T. & Tibshirani, R. (2013), ‘A sparse-group lasso’, *Journal of*  
293 *Computational and Graphical Statistics* **22**(2), 231–245.  
294 **URL:** <https://doi.org/10.1080/10618600.2012.681250>
- 295 Sudlow, C., Gallacher, J., Allen, N., Beral, V., Burton, P., Danesh, J., Downey, P., Elliott, P.,  
296 Green, J., Landray, M., Liu, B., Matthews, P., Ong, G., Pell, J., Silman, A., Young, A., Sprosen,  
297 T., Peakman, T. & Collins, R. (2015), ‘Uk biobank: An open access resource for identifying the  
298 causes of a wide range of complex diseases of middle and old age’, *PLOS Medicine* **12**(3), 1–10.  
299 **URL:** <https://doi.org/10.1371/journal.pmed.1001779>

- 300 Tibshirani, R. (1996), ‘Regression shrinkage and selection via the lasso’, *Journal of the Royal Sta-*  
301 *tistical Society. Series B (Methodological)* **58**(1), 267–288.  
302 **URL:** <http://www.jstor.org/stable/2346178>
- 303 Tibshirani, R., Bien, J., Friedman, J., Hastie, T., Simon, N., Taylor, J. & Tibshirani, R. J. (2012),  
304 ‘Strong rules for discarding predictors in lasso-type problems’, *Journal of the Royal Statistical*  
305 *Society. Series B (Statistical Methodology)* **74**(2), 245–266.  
306 **URL:** <http://www.jstor.org/stable/41430939>
- 307 Yuan, M. & Lin, Y. (2006), ‘Model selection and estimation in regression with grouped variables’,  
308 *Journal of the Royal Statistical Society Series B* **68**, 49–67.